Journal of Clinical and Translational Hepatology **2022**
DOI: 10.14218/JCTH.2022.00005

Original Article

Upregulation of GLT25D1 in Hepatic Stellate Cells Promotes Liver Fibrosis via the TGF-β1/SMAD3 Pathway *In Vivo* and *In vitro*

Shiwei Wang[1#], Lingling He[1#], Fan Xiao[2], Meixin Gao[1], Herui Wei[1], Junru Yang[1], Yang Shu[1], Fuyang Zhang[1], Xiaohui Ye[3], Ping Li[1], Xiaohua Hao[4], Xingang Zhou[5] and Hongshan Wei[1,6]

[1]Department of Gastroenterology, Beijing Ditan Hospital, Capital Medical University, Beijing, China; [2]Institute of Infectious Diseases, Beijing Ditan Hospital, Capital Medical University, Beijing, China; [3]Department of Gastroenterology, Beijing Huaxin Hospital, the First Affiliated Hospital of Tsinghua University, Beijing, China; [4]Beijing Ditan Hospital, Capital Medical University, Beijing, China; [5]Department of Pathology, Beijing Ditan Hospital, Capital Medical University, Beijing, China; [6]Department of Gastroenterology, Peking University Ditan Teaching Hospital, Beijing, China

Received: 4 January 2022 | **Revised:** 23 March 2022 | **Accepted:** 12 April 2022 | **Published:** 26 May 2022

Abstract

Background and Aims: Collagen β(1-O) galactosyltransferase 25 domain 1 (GLT25D1) is associated with collagen production and glycosylation, and its knockout in mice results in embryonic death. However, its role in liver fibrosis remains elusive, particularly in hepatic stellate cells (HSCs), the primary collagen-producing cells associated with liver fibrogenesis. Herein, we aimed to elucidate the role of GLT25D1 in HSCs. ***Methods:*** Bile duct ligation (BDL)-induced mouse liver fibrosis models, primary mouse HSCs (mHSCs), and transforming growth factor beta 1 (TGF-β1)-stimulated LX-2 human hepatic stellate cells were used in *in vivo* and *in vitro* studies. Stable LX-2 cell lines with either GLT25D1 overexpression or knockdown were established using lentiviral transfection. RNA-seq was performed to investigate the genomic differences. HPLC-MS/MS were used to identify glycosylation sites. Scanning electronic microscopy (SEM) and second-harmonic generation/two-photon excited fluorescence (SHG/TPEF) were used to image collagen fibril morphology. ***Results:*** GLT25D1 expression was upregulated in nonparenchymal cells in human cirrhotic liver tissues. Meanwhile, its knockdown attenuated collagen deposition in BDL-induced mouse liver fibrosis and inhibited mHSC activation. GLT25D1 was overexpressed in activated versus quiescence LX-2 cells and regulated *in vitro* LX-2 cell activation, including proliferation, contraction, and migration. GLT25D1 also significantly increased liver fibrogenic gene and protein expression. GLT25D1 upregulation promoted HSC activation and enhanced collagen expression through the TGF-β1/SMAD signaling pathway. Mass spectrometry showed that GLT25D1 regulated the glycosylation of collagen in HSCs, affecting the diameter of collagen fibers. ***Conclusions:*** Collectively, the upregulation of GLT25D1 in HSCs promoted the progression of liver fibrosis by affecting HSCs activation and collagen stability.

Citation of this article: Wang S, He L, Xiao F, Gao M, Wei H, Yang J, *et al*. Upregulation of GLT25D1 in Hepatic Stellate Cells Promotes Liver Fibrosis via the TGF-β1/SMAD3 Pathway *In Vivo* and *In vitro*. J Clin Transl Hepatol 2022. doi: 10.14218/JCTH.2022.00005.

Introduction

Liver fibrosis is caused by various chronic liver diseases, can progress to cirrhosis and hepatocellular carcinoma, and it is associated with significant morbidity and mortality.[1,2] However, the molecular mechanisms underlying the condition are complex and not fully understood. Apart from etiological treatments, there are no direct antiherpetic fibrosis therapeutics, thus additional research is required.

Liver fibrosis characterized by the accumulation of proteins in the extracellular matrix (ECM) following the activation and proliferation of hepatic stellate cells (HSCs).[3] Changes in collagen are the most important ECM changes associated with fibrogenesis and fibrinolysis.[4] Many post-translational modifications occur during procollagen biosynthesis in the rough endoplasmic reticulum (rER), facilitating proper collagen folding, secretion, and biological functions.[5] Of these modifications, proline and lysine hydroxylation are well-recognized and studied.[6,7] However, collagen glycosylation has not been extensively investigated.

In 1935, Grassmann and Schleich first described collagen glycosylation. Approximately 30 years later, Spiro described the glycan structure: Glc(α1-2) Gal(β1-O) Hyl.[8] The corresponding glycosyltransferase enzymes collagen β(1-O) galactosyltransferase 1 (GLT25D1) and collagen

Keywords: Collagen; Glycosylation; Hepatic stellate cells; Liver fibrosis; TGF-β1.

Abbreviations: BDL, Bile duct ligation; CCN1, Cellular communication network factor 1; CoL, collagen; GLT25D1, Collagen β(1-O) galactosyltransferase 25 domain 1; HSCs, hepatic stellate cells; mHSCs, primary mouse HSCs; TGF-β1, transforming growth factor beta 1; WT, wild-type.

[#]Contributed equally to this work

[*]**Correspondence to:** Hongshan Wei, Department of Gastroenterology, Beijing Ditan Hospital, Capital Medical University, No. 8, Jingshun East Street, Chaoyang District; Department of Gastroenterology, Peking University Ditan Teaching Hospital, Beijing 100015, China. ORCID: https://orcid.org/0000-0001-8893-653X. Tel: +86-10-84322521, Fax: +86-10-84322130, E-mail: drwei@ccmu.edu.cn

β(1-O) galactosyltransferase 2 (GLT25D2) were identified by Schegg *et al.* in 2009.[9] GLT25D1 adds glucosylgalactosyl-hydroxylysine (GG-Hyl) or galactosyl-hydroxylysine (G-Hyl) to specific procollagen hydroxylysine molecules prior to the formation of the triple helix structure in the endoplasmic reticulum (ER).[9–11] GLT25D1 regulates cross-linking in bone collagen I.[12] Knocking out GLT25D1 in osteosarcoma SaOS-2 cells impaired cell proliferation and viability and induced the upregulation and intracellular accumulation of collagen I.[13] In MC3T3-E1 preosteoblast cells, loss of GLT25D1 affects the maturation of collagen cross-linking, fibrillogenesis, and mineralization of collagen fibrils.[14] In N-ethyl-N-nitrosourea (ENU)-induced mutant mice carrying a *GLT25D1* mutation, collagen IV accumulates inside embryonic fibroblasts and within the ECM.[15] GLT25D1 also decreases adiponectin secretion in early obesity and is associated with cerebral small vessel disease through its effect on COL4A1,[16,17] indicating that it has a vital role in collagen fibrillogenesis, cross-linking, mineralization, and collagen-cell interaction.[12]

In light of the findings, we hypothesized that GLT25D1 may play an essential role in activating HSCs, the primary collagen-producing cells associated with liver fibrosis. We used GLT25D1-knockout (KO) mice (C57BL/6J) to investigate this role. However, knocking out GLT25D1 was lethal to the embryos.[18] Therefore, heterozygous GLT25D1$^{+/-}$ mice, obtained using Cre-loxP conditional knockout technique, were used. Modeling studies suggest that GLT25D1 may play a role in acute hepatic injury and liver fibrosis.[18,19] GLT25D2 deficiency contributes to lipodystrophy and promotes NAFLD.[20] We previously showed that GLT25D1 has an essential role in liver disease, although its role and underlying mechanism in liver fibrosis are still poorly understood.

In this study, we demonstrated the role of GLT25D1 in primary mouse HSCs and LX-2 cells for the first time. We found that GLT25D1 was upregulated in activated HSCs and played an essential role in HSC activation. GLT25D1 also potentially affected collagen stability. The results suggest that GLT25D1 is a novel and potential antifibrotic target.

Methods

Human liver samples

This study was approved by the Institutional Ethics Committee of the Beijing Ditan Hospital. Written informed consent was obtained from all patients prior to obtaining liver samples. Liver samples were collected from eight patients with chronic hepatitis B who underwent hepatic surgery or liver puncture biopsy at Beijing Ditan Hospital between June and November 2020. Three of the patients had mild chronic portal inflammation (S0–S1, control) and five patients had cirrhosis. All biopsy specimens were histologically scored via blinded assessment using the Ishak system.[21] Patient baseline information is shown in Supplementary Table 1.

Bile duct ligation (BLD)-induced liver fibrosis

The experimental Animal Welfare Committee of Capital Medical University approved all animal procedures. We used GLT25D1$^{+/-}$ mice, which were generated as previously described.[18,19] 6–8-week-old male C57BL/6J wild-type (WT) and GLT25D1$^{+/-}$ mice were anesthetized via intraperitoneal injection with 0.8% pentobarbital. After a scalpel midline laparotomy, the liver lobules were turned down and the intestines exteriorized carefully to expose the bile duct. The common bile duct was ligated twice using 6–0 silk sutures and the abdomen was then closed. A sham operation was performed in a similar manner, except that the bile duct was not ligated. The animals were sacrificed on postoperative day 21 and the plasma and liver samples were collected for further experiments.

Hepatic hydroxyproline assay

The total collagen content was assessed by measuring hydroxyproline levels in liver tissue using the kit (Nanjing Jiancheng Bioengineering Institute, Nanjing, China).

Insoluble collagen content assay

The concentration of insoluble collagen (cross-linked collagen) in liver tissue was measured using Biocolor Sircol insoluble collagen assay kits (Biocolor Ltd., Carrickfergus, UK).[22] Briefly, 20–30 mg (wet weight) of liver samples were crushed in the fragmentation reagent, incubated at 65°C for 2–3 h, and the supernatant was collected and stained for 30 m using Sircol dye reagent. An acid salt wash was used to remove unbound dye and an alkali reagent was then added to release the collagen-bound dye into the solution using a vortex mixer. Absorbance was measured at 550 nm within 2–3 h of the reaction.

Isolation of primary mouse HSCs

Primary mouse hepatic stellate cells (mHSCs) were isolated from 8–10-week-old male C57BL/6J WT and GLT25D1$^{+/-}$ mice by enzymatic digestion and OptiPrep density gradient centrifugation.[23] Briefly, each liver was first perfused *in situ* through the hepatic portal vein using pronase, DNase I, and type IV collagenase. The liver was then excised, homogenized, and digested in external digestive fluid. The mixture was filtered through a 100 μm mesh and centrifuged at 450×*g* for 7 m. The supernatant was discarded and the cell pellet resuspended in 5 mL of 15% OptiPrep (Sigma-Aldrich, St Louis, MO, USA) and slowly loaded with 5 mL of 11.5% OptiPrep and then 5 mL Gey's balanced salt solution (GBSS). After centrifuging at 1,400×*g* and 4 °C for 17 m, the mHSC layer (white flocculus) between the 11.5% OptiPrep and the GBSS was transferred into a new tube, mixed with GBSS, and centrifuged at 450×*g* for 7 m. The cell pellet was resuspended in Dulbecco's modified Eagle medium (DMEM) supplemented with 10% fetal bovine serum (FBS). Primary hepatic stellate cells from two mice of the same group were pooled as one sample. The purity of primary HSCs was determined by adding Oil Red O staining to freshly isolated primary cells that had been cultured for 2 days (>97%).[24] HSC viability was determined using the Trypan blue exclusion test (>90%). Isolated mHSCs were cultured in DMEM supplemented with 10% FBS at 37°C in a 5% CO_2 atmosphere. Activated mHSCs were obtained 7 days after the initial culture.

Immunohistochemistry (IHC) and Immunofluorescence (IF) assays

Human and mouse liver tissues were fixed in 10% neutral buffered formalin and embedded in paraffin and then divided into 4 μm thick sections. Immunohistochemistry assays

were conducted using the liver tissue sections. Tissue slides were deparaffinized, hydrated, incubated with 10% H_2O_2 for 10 m and then steamed in 0.01 mol/L citrate sodium buffer for 30 m. The reaction was blocked by adding 2% bovine serum albumin (BSA) and incubating for 1 h at room temperature. After blocking, a 1:100 dilution of anti-rabbit GLT25D1 antibody was added and the reaction incubated overnight at 4°C. The following day, the slides were washed three times with phosphate buffered saline (PBS) and then incubated with goat anti-rabbit antibody for 1 h at room temperature. Immunoreactive signals were visualized for 5 m using 3,3′-diaminobenzidine.

The cells were grown on 25 mm sterile cell climbing slices for 7 days and then fixed in 4% paraformaldehyde for 15 m at room temperature. After washing three times with PBS, the cells were incubated with 5% BSA for 1 h and then with primary antibody (mouse anti-collagen type I 1:200; Servicebio, Hubei, China) overnight at 4°C. After washing with PBS, the cells were incubated with secondary antibody (CY3; Servicebio, Hubei, China) for 1 h at room temperature. Cell nuclei were stained using diamidino-phenylindole (Biotium, Hayward, CA, USA). Images were acquired using the same microscope parameters (Nikon, Tokyo, Japan) and analyzed using ImageJ software.

Second-harmonic generation/two-photon excited fluorescence (SHG/TPEF) imaging

SHG/TPEF microscopy is a novel optical tissue imaging system that can be used to characterize fibrillar collagen and analyze pathology-relevant collagen architectural features.[25,26] Four micron-thick unstained sections of mouse liver tissues were anonymized and imaged at HistoIndex Pte Ltd (Singapore). Four morphological features were investigated: the number of short strings (length ≤20 μm), the number of long strings (length >20 μm), the number of thin strings (axis ratio ≤0.25), and the number of thick strings (axis ratio >0.25).

Generation of plasmid constructs and LX-2 single cell-derived clones

Briefly, the lentiviral expression vectors GLT25D1-Plvx-shRNA2-Zsgreen-T2A-puro (Fig. 1E) and GLT25D1-pCDH-CMV-MCS-EF1-GFP-T2A-Puro (Fig. 2A) were successfully constructed at Generay biotech (Beijing, China) and confirmed by sequence analysis. Lentiviruses containing these vectors were prepared and transfected into LX-2 cells using FuGENE 6 transfection reagent (Roche, Basel, Switzerland). Then, single cell-derived clones stably suppressing GLT25D1 (sh-GLT25D1), overexpressing GLT25D1 (OE-GLT25D1), and corresponding negative controls (NC) were selected by subjecting the cells to 2 μg/mL puromycin treatment for one week. Successful section was confirmed using western blot and Quantitative real-time polymerase chain reaction (qPCR).

RNA sequencing and data analysis

Two biological replicates from each mouse group (WT and GLT25D1$^{+/-}$) and three biological replicates from each clonal group (OE-NC and OE-GLT25D1) were pooled and sequenced on the Illumina NovaSeq 6000. Differential gene expression between the two groups was analyzed using the DESeq2 R package (1.20.0). padj ≤ 0.05 and $|\log_2$ (fold change)| ≥1 were set as thresholds for significant differential expression. The ClusterProfiler R package (3.8.1) was used to conduct gene ontology (GO) enrichment analysis of the differentially expressed genes.

Cell culture and treatment

The human hepatic stellate cell line LX-2 (Institute of Infectious Diseases, Beijing Ditan Hospital) was cultured in DMEM (Gibco, Waltham, MA, USA) with 10% FBS and 1% penicillin/streptomycin (Solarbio, Beijing, CN) at 37°C in a humidified atmosphere containing 5% CO_2. The LX-2 cells were starved in serum-free DMEM for 12 h prior to commencing the experiments. Transforming growth factor β1 (TGF-β1, 10 ng/mL), a robust fibrosis mediator, was used to stimulate LX-2 cells to simulate liver fibrosis formation. The control group was treated with the same volume of vehicle. Specific signal pathway inhibitors: SIS3 and SD208 (MedChemExpress, Monmouth Junction, NJ, USA), were added 1 h before adding TGF-β1.

Cell proliferation assay

Cell proliferation was measured using the Cell Counting Kit-8 (Dojindo, Kumamoto, Japan) assay following the manufacturer's protocol. Briefly, LX-2 stable and control cells were seeded in 96-well plates at 2–5×10^3 cells per well for 12 h and then induced with 10 ng/mL TGF-β1. Thereafter, 10 μL of CCK8 solution was added to each well. Cell growth curves were generated based on optical density absorbance measured at 450 nm using a Varioskan Flash spectrophotometer (Thermo Fisher Scientific, Waltham, MA, USA).

Wound healing cell migration assay

A wound healing cell migration assay was used to study directional cell migration *in vitro.*[27] Cells were seeded in 12-well culture dishes and cultured for 24 h. The cells were then treated with 10 ng/mL TGF-β1 and scratched with a 10 μL pipette tip. Images were captured under a microscope immediately following wound creation (0 h) and photos were taken every 24 h for 3 days. Images were analyzed in ImageJ and the percentage wound migration area determined.

Cell contraction assay

A standard assay kit (Cell Biolabs, San Diego, CA, USA) was used. LX-2 cells were harvested and resuspended in DMEM. Two parts of the cell suspension was mixed with eight parts of the collagen gel lattice mixture and plated for 1 h at 37°C. After gel polymerization, 1 mL of the medium was added and the mixture incubated for 2 days. Next, 1 mL medium containing TGF-β1 was added and the gels released from the sides of the wells. Images were obtained after 24 h. The changes in collagen gel sizes were analyzed using ImageJ software and normalized to the area of the well.

RNA extraction and quantitative real-time PCR analysis

Total RNA was extracted from cells or tissues using an animal tissue cell total RNA extraction kit (BioSci, Beijing, China), following the manufacturer's protocol. cDNA was prepared using a PrimeScript RT reagent kit (Takara, Kyoto, Japan), following the manufacturer's instructions. qPCR was

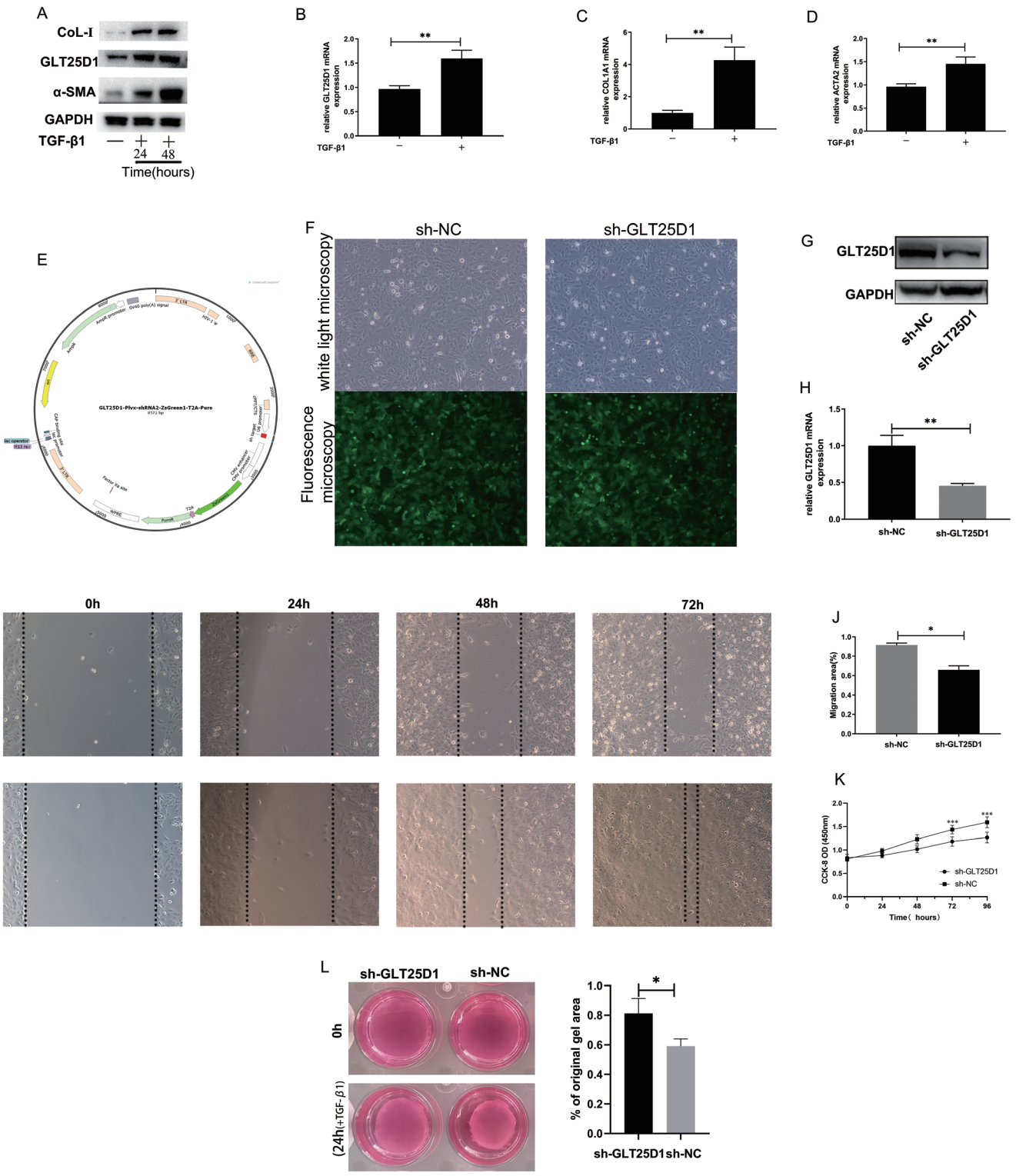

Fig. 1. Knocking down GLT25D1 inhibits the activation of LX-2 cells and their corresponding phenotypes. (A) Western blot assay showing the expression of COL I, α-SMA, and GLT25D1 proteins following 24 h and 48 h of stimulation with transforming growth factor beta 1 (TGF-β1). (B–D) RT-PCR assay of *COL 1A1, ACTA2*, and *GLT25D1* extracted from LX-2 cells following 48 h of stimulation with TGF-β1. (E) Lentiviral expression vector GLT25D1-Plvx-shRNA2-Zsgreen-T2A-puro. (F) Representative images of sh-NC and sh-GLT25D1 cells stably transfected with fluorescence-labeled lentiviruses viewed under bright-field and fluorescence microscopy. (G) Western blot analysis of the knockdown efficiency of GLT25D1 in sh-GLT25D1 cells. (H) Real-time PCR assay of the knockdown efficiency of GLT25D1 in LX-2 cells. (I, J) LX-2 cell wound healing assay. (K) Assessment of cell proliferation using CCK-8 assays. (L) Collagen gel contraction. Representative results from three independent experiments are shown. Data are means±SD. NS, not significant; *,<0.05; **,<0.01; ***,<0.001.

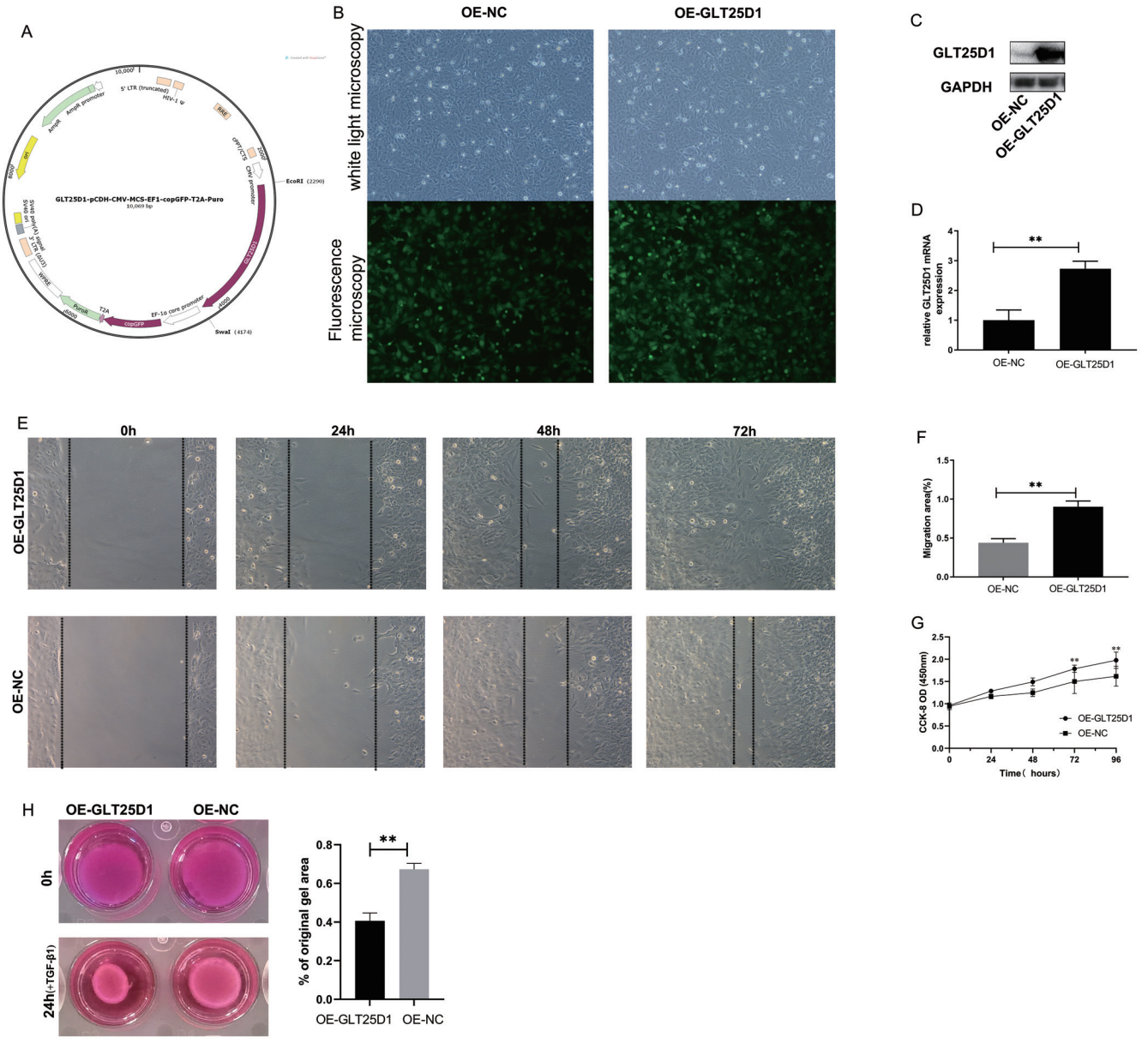

Fig. 2. GLT25D1 overexpression activates LX-2 cells and their corresponding phenotypes. (A) Lentiviral expression vector GLT25D1-pCDH-CMV-MCS-EF1-copGFP-T2A-Puro. (B) Representative images of OE-NC and NC-GLT25D1 cells stably transfected with fluorescence-labeled lentivirus viewed under white light and fluorescence microscopy. (C) Western blot analysis of the overexpression efficiency of GLT25D1 in LX-2 cells. (D) Real-time PCR assay of the overexpression efficiency of GLT25D1 in LX-2 cells. (E, F) LX-2 cell wound healing assay. (G) Assessment of cell proliferation using CCK-8 assays. (H) Collagen gel contraction. Representative results from three independent experiments are shown. Data are means±SD. NS, not significant; *,<0.05; **,<0.01; ***,<0.001.

performed using Fast SYBR Green PCR Master Mix (Applied Biosystems, Waltham, MA, USA). Transcript levels were analyzed using the ΔΔCT method and normalized to that of the internal control gene, glyceraldehyde-3-phosphate dehydrogenase. Each reaction was performed in triplicate and each experiment was performed at least three times. The primers used in this study are listed in Supplementary Table 2.

Protein extraction and western blot assay

Cells or mouse liver tissues were lysed using RIPA buffer supplemented with protease inhibitor (Roche) and phosphatase inhibitor cocktails 2 and 3 (Sigma). Protein concentrations were measured using a bicinchoninic acid assay kit (Thermo Scientific, Waltham, MA, USA). Proteins were separated on a 10% gel and transferred onto 0.2 μm polyvinylidene difluoride membranes (SDS-PAGE; Millipore, Darmstadt, Germany). After blocking with 5% skimmed milk and washing with TBS-Tween buffer, the membranes were incubated overnight at 4°C with the corresponding antibodies (Supplementary Table 3). The membranes were then incubated with a horseradish peroxidase-conjugated secondary antibody (1:5,000) (ZSGB-bio) for 1 h at room temperature and then with an enhanced chemilumines-

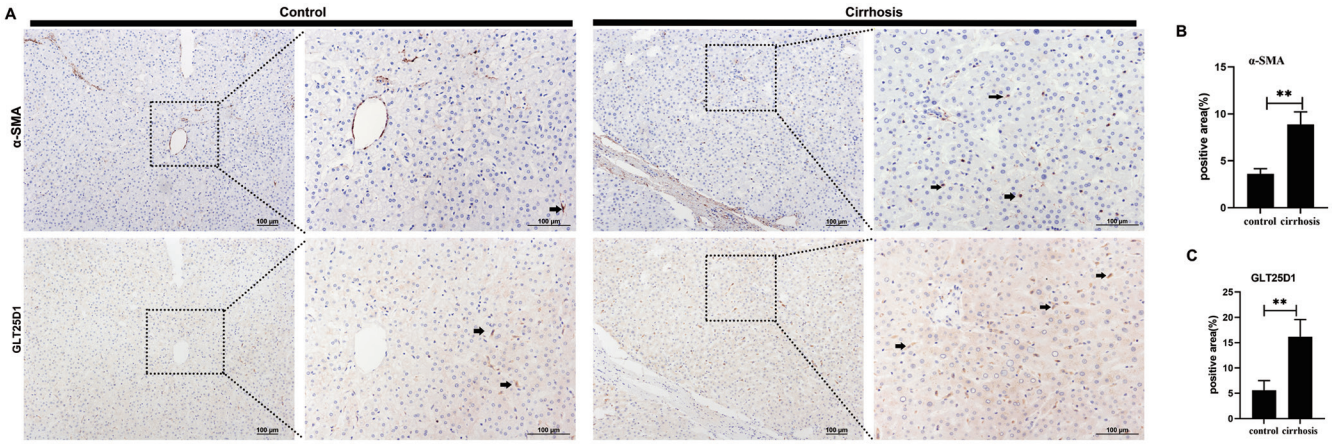

Fig. 3. Collagen β(1-O) galactosyltransferase 25 domain 1 (GLT25D1) is upregulated in the cirrhotic liver and is present in nonparenchymal cells. (A) Tissue sections from cirrhotic and normal (control) patient livers were analyzed using immunohistochemistry assays. Representative images are shown. The black arrow indicates α-SMA and GLT25D1 positive cells. (B) α-SMA positive area (%). (C) GLT25D1 positive area (%). Representative results from three independent experiments are shown. Data are means±SD. NS, not significant; *,<0.05; **,<0.01; ***,<0.001.

cence substrate (Millipore, Darmstadt, Germany). Relative protein quantities were determined using ImageJ software. Information on the antibodies is presented in Supplementary Table 3.

Mass spectrometry-based identification of glycosylated Hyl residues

Proteins were extracted from lysates of activated sh-GLT25D1, OE-GLT25D1, and control cells. Type I collagen was separated by SDS-PAGE on 10% Bis-Tris precast gels. After staining with Coomassie SimplyBlue, the target protein band was excised from the gel using a scalpel. The bands were cut and diced into 1 mm^3 cubes, digested with trypsin, and subjected to mass spectrometry analysis. HPLC-MS/MS analyses were conducted using a RIGOL L-3000 HPLC system (RIGOL, Beijing, China). The MS scan was obtained over a 500−2,000 m/z range with a 2 Hz frequency in positive ion mode. Peptides were identified by searching the acquired MS/MS spectra against *Homo sapiens* database using the Proteome Discoverer 2.4 software.

Characterization of collagen fibrils using scanning electron microscopy

Specimens were sampled from the same areas of the liver and fixed using an electron microscope fixation liquid (Solarbio, Beijing, China). The samples were then post-fixed in potassium ferrocyanide-reduced osmium for 1 h at room temperature. Collagen fibrils were observed under a scanning electron microscope. The diameters (μm) of collagen fibers were measured in three different fields of view using Image-Pro Plus software (version 6.0; Media Cybernetics Inc., Rockville, MD, USA).

Statistical analysis

Data were reported as percentages (%) or means±SD of at least three independent experiments. Statistical analyses were performed using Prism 9 software (GraphPad, La Jolla, CA, USA). Pairwise comparisons between groups were performed using unpaired Student's *t*-test. The χ^2 test was used to analyze pathological characteristics. For p-values, <0.05, <0.01, and <0.001 were considered statistically significant.

Results

GLT25D1 protein is upregulated in the cirrhotic liver and present in nonparenchymal cells

We initially investigated GLT25D1 expression in human liver tissue. α-SMA and GLT25D1 levels were significantly elevated in cirrhotic livers compared with the control livers without fibrosis (Fig. 3A–C). GLT25D1 and α-SMA, a marker of activated HSCs in fibrotic livers, were mainly expressed in nonparenchymal cells (Fig. 3A), suggesting a potential role for GLT25D1 in liver fibrosis and HSCs.

GLT25D1 downregulation attenuates collagen deposition

We used heterozygous GLT25D1$^{+/-}$ and WT mice subjected to BDL-induced liver fibrosis to further investigate the *in vivo* role of GLT25D1 in liver fibrosis. Sirius Red staining and immunohistochemical analysis of α-SMA showed that GLT25D1$^{+/-}$ mice had reduced collagen deposition compared with WT mice (Fig. 4A), in line with decreased hydroxyproline levels (Fig. 4B). The expression of fibrotic genes, including *COL1A1*, *COL3A1*, and *ACTA2*, was significantly downregulated in GLT25D1$^{+/-}$ mice compared with WT mice (Fig. 4C). The GLT25D1 protein levels in liver was provided in the Supplementary Figure 1. The results demonstrate that GLT25D1 knockdown attenuates BDL-induced liver fibrosis *in vivo*.

GLT25D1 downregulation inhibits primary HSC activation and collagen expression

IHC results from the analysis of human and mouse liver tissues indicated that GLT25D1 was mainly expressed in non-parenchymal cells. HSCs, which are non- parenchymal cells, are the primary collagen-producing cells and key effectors

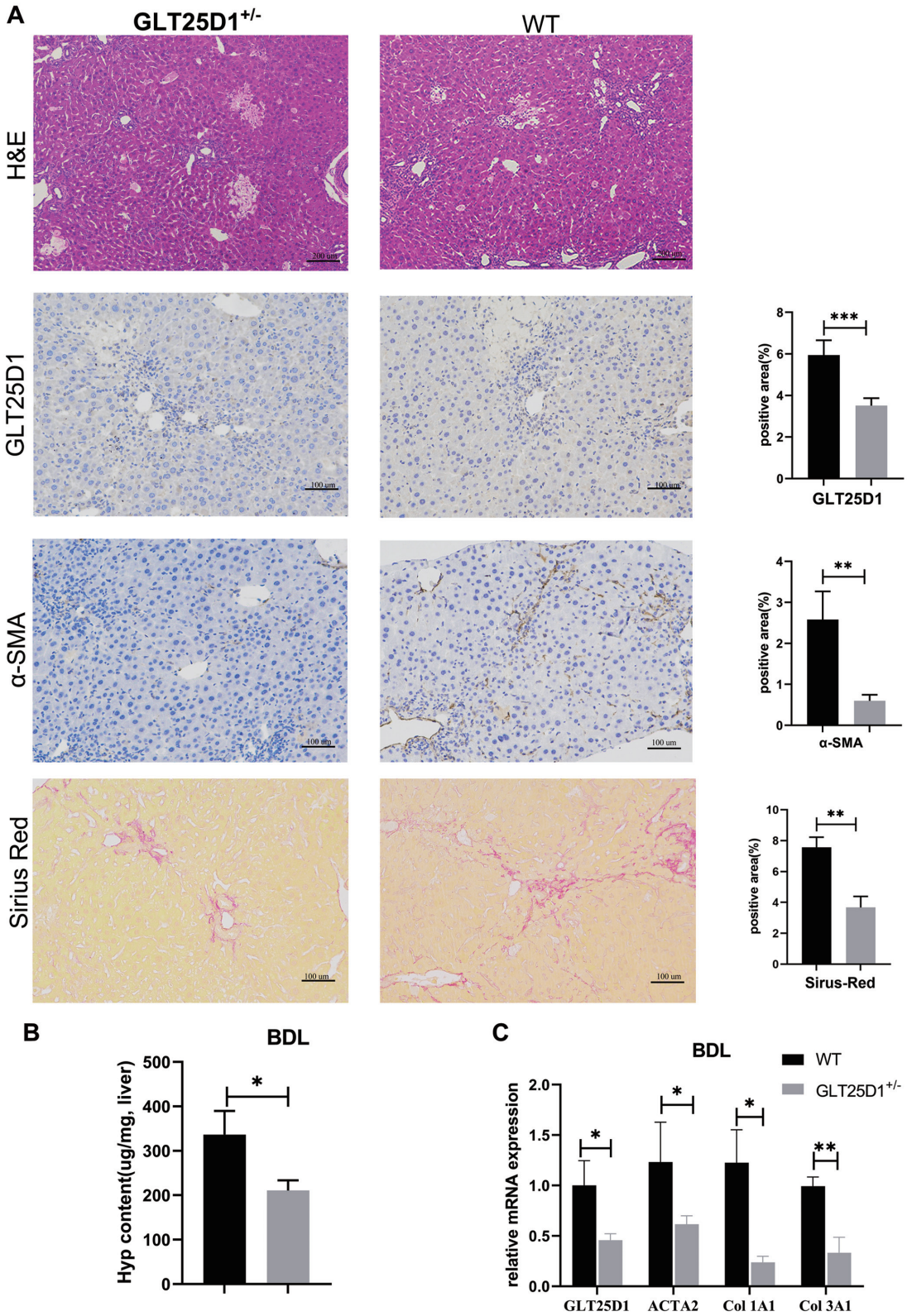

Fig. 4. GLT25D1 downregulation attenuates Bile duct ligation (BLD) -induced liver fibrosis. (A) Representative histological sections of GLT25D1$^{+/-}$ and wild-type (WT) male mice livers stained using hematoxylin and eosin, Sirius Red, and immunohistochemicals (GLT25D1 and α-SMA). Quantification of positive staining areas, measured by Image J software, are shown in the right panels. (B) Hydroxyproline content in the liver tissues (n=6). (C) RT-PCR assay of fibrotic genes. Representative results from three independent experiments are shown. Data are means±SD; NS, not significant; *,<0.05; **,<0.01; ***,<0.001.

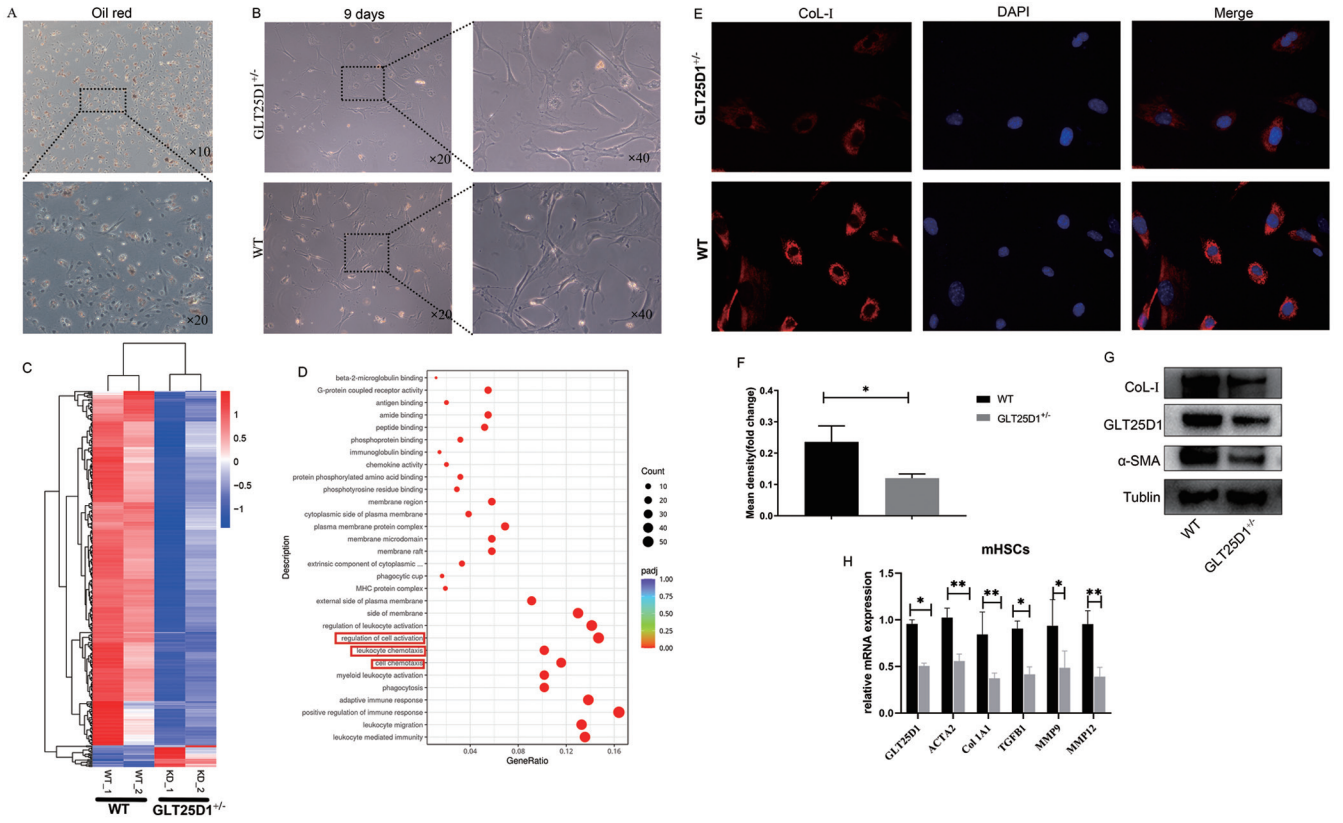

Fig. 5. Knocking down GLT25D1 inhibits murine hepatic stellate cell (mHSC) activation and collagen expression. (A) Oil red staining of mHSCs that have been cultured for 2 days. (B) Morphology of mHSCs that have been cultured for 9 days. (C) Heatmap of differentially expressed mHSC genes from WT and GLT25D1$^{+/-}$ mice (mHSCs were cultured for 12 days). Blue represents low expression and red represents high expression. (D) Scatter plot of Kyoto Encyclopedia of Genes and Genomes enrichment analysis of differentially expressed genes. The top 10 significant GO enrichments are shown. (E) Immunofluorescent staining of COL I in mHSCs from WT and GLT25D1$^{+/-}$ mice (mHSCs were cultured for 12 days). (F) Mean fluorescence density of COL I. (G) Western blots showing the levels of COL I, α-SMA, and GLT25D1 proteins in mHSCs lysates from WT and GLT25D1$^{+/-}$ mice (mHSCs were cultured for 10 days). (H) RT-PCR assay of the fibrotic genes *COL1A1, COL3A1,* and *GLT25D1* in LX-2 cells following 48 h of stimulation with TGF-β1. Representative results from three independent experiments are shown. Data are means±SD. NS, not significant; *,<0.05; **,<0.01; ***,<0.001.

of liver fibrosis. Therefore, based on the hypothesis that GLT25D1 regulates HSCs in liver fibrosis, we isolated primary HSCs from WT and GLT25D1$^{+/-}$ mouse livers. Quiescent mHSCs showed characteristic lipid droplets (Fig. 5A). mHSCs were activated when the cells were cultured for 9 days, resulting in a spindle-shaped or dendritic morphology (Fig. 5B, left panels). mHSC from WT mice showed more obvious stress fiber-like structures compared with GLT25D1$^{+/-}$ mice after 9 days of culture (Fig. 5B, right panels).

To further explore the effects of GLT25D1 on HSCs, RNA-seq analysis of mHSCs from WT and GLT25D1$^{+/-}$ mice was performed after culturing the cells for 12 days. A total of 360 significantly downregulated genes and 22 significantly upregulated genes were identified (Fig. 5C). The expression of fibrosis-related genes was significantly lower in mHSCs from GLT25D1$^{+/-}$ mice compared with those from WT mice, including transforming growth factor beta (TGFβ1), matrix metallopeptidase 9 (MMP9), and MMP12. GO analysis suggested that the genes that were differentially expressed between GLT25D1$^{+/-}$ and control WT mice were associated with cell activation and corresponding downstream profibrogenic responses, including cell chemotaxis and activation (Fig. 5D).[28] Immunofluorescence analysis showed that knocking down GLT25D1 reduced intracellular COL I protein levels (Fig. 5E, F). Western blot and RT-PCR results also confirmed that knocking down GLT25D1 in mHSCs significantly decreased α-SMA and intracellular COL I protein levels (Fig. 5G, H). Taken together, these results show that GLT25D1 may be involved in mHSC activation and ECM production.

GLT25D1 knockdown inhibits the activation of LX-2 cells and their corresponding phenotypes

To further assess the effects of GLT25D1 on HSCs, the human hepatic stellate cell line LX-2, which is commonly used in *in vitro* hepatic fibrosis studies, was employed. Primary HSCs and LX-2 cells share high gene expression similarities (98.7%).[29,30] Western blot analysis revealed that the fibrosis-associated proteins COL I, α-SMA, and GLT25D1 protein were upregulated in activated LX-2 cells (Fig. 1A). qRT-PCR also showed that *COL1A1, ACTA2,* and *GLT25D1* mRNA levels were significantly elevated (Fig. 1B–D). The results demonstrate that GLT25D1 expression was upregulated at both mRNA and protein levels following the TGF-β1-induced activation of LX-2 cells. Thus, GLT25D1 may be involved in LX-2 cell activation and ECM production.

Additionally, we constructed a lentivirus vector expressing shGLT25D1 (Fig. 1E) and generated a stable cell line (shGLT25D1, Fig. 1F) that successfully knocked down GLT25D1 gene expression (63.2%) than control (Fig. 1G, H). HSC activation is accompanied by specific phenotypes, including proliferation, contractility, and migration.[28] The wound

healing assay indicated that knocking down GLT25D1 inhibited LX-2's migratory capacity ($p<0.05$, Fig. 1I, J). The CCK-8 assay showed that the viability of sh-GLT25D1 cells decreased significantly compared with that of sh-NC cells (Fig. 1K). Collagen gel contraction was used to determine whether GLT25D1 affects HSC contractility. The results showed that knocking down GLT25D1 repressed TGF-β1-induced LX-2 contraction ($p<0.05$, Fig. 1L), indicating that suppressing GLT25D1 may affect LX-2 cell activation.

GLT25D1 overexpression promotes the activation of LX-2 cells and their corresponding phenotypes

Based on the results, we postulated that GLT25D1 is involved in LX-2 cell activation. Rescue experiments were performed to confirm these results by testing whether GLT25D1 overexpression has opposite effects in LX-2 cells, including increased cell proliferation, contractility, and migration. We constructed a GLT25D1 overexpressing lentivirus vector (Fig. 2A) and generated cell lines that stably overexpress GLT25D1 (OE-GLT25D1, Fig. 2B), showing high expression of GLT25D1 protein (260%) and mRNA (173%) compared with the OE-NC control (Fig 2C, D). The results showed that GLT25D1 overexpression increased migratory capacity and promoted cell proliferation (Fig. 2E–G) in OE-GLT25D1 compared with the control. GLT25D1 overexpression also enhanced LX-2 cell contraction (Fig. 2H). Taken together, these results confirm that GLT25D1 may mediate LX-2 cell activation.

GLT25D1 regulates TGF-β1-induced ECM production by LX-2 cells

To elucidate the effects of GLT25D1 overexpression in LX-2 cells, RNA-seq analysis was conducted in OE-GLT25D1 and OE-NC cells 48 h after their stimulation with TGF-β1. The analysis identified 512 upregulated and 167 downregulated genes (Fig. 6A). The expression of fibrosis-related genes, including *COL1A2, COL3A1, ACTA2, TIMP3, PDGFRA, COL11A1, CAV1*, and *IGFBP3* was significantly upregulated in OE-GLT25D1 cells compared with OE-NC cells. GO enrichment analysis was performed to further explore the biological functions of the DEGs. GLT25D1 greatly affected ECM and collagen formation (Fig. 6B). Western blot and RT-PCR verified the accuracy of the transcriptome data. Western blot results showed that the expression of α-SMA (a marker of LX-2 activation), COL I, COL III, and TIMP-1 were suppressed in sh-GLT25D1 (Fig. 6C-G) but activated in OE-GLT25D1 cells (Fig. 6H-L). Expression of the corresponding liver fibrogenic genes: *COL1A2, COL3A1, ACTA2*, and *TIMP-1,* showed similar patterns in sh-GLT25D1 (Fig. 6M–P) and OE-GLT25D1 cells (Fig. 6Q-T) 48 h after they were stimulated with TGF-β1. Taken together, these results indicate that GLT25D1 is required, to some extent, for the activation and expression of fibrogenic genes in LX-2 cells.

GLT25D1 drives ECM production through the TGF-β1/SMAD3 signaling pathway

The canonical TGF-β/SMAD pathway and noncanonical pathway (MAPK, PI3K/AKT) were evaluated to study the mechanisms of action of GLT25D1. GLT25D1 knockdown decreased TGFβ1-stimulated SMAD3 phosphorylation (Fig. 7A), whereas GLT25D1 overexpression enhanced TGFβ1-stimulated SMAD3 phosphorylation (Fig. 7B). There was no significant difference in noncanonical pathway. Thus, we hypothesized that GLT25D1 regulated activation and ECM production of LX-2 cells via the TGF-β1/SMAD3 signaling pathway. Smad3 phosphorylation inhibitor (SIS3) and TGF-βRI (ALK5) inhibitor (SD208) were used to confirm whether GLT25D1 regulated LX-2 activation by arresting the TGF-β/SMAD3 signaling pathway.[31] Western blot analysis showed that SIS3 and SD208 significantly suppressed GLT25D1-induced collagen synthesis and completely abrogated collagen upregulation (Fig. 7C). The results suggest that GLT25D1 promotes the expression of fibrogenic proteins during liver fibrosis through the TGF-β1/SMAD3 signaling pathway.

GLT25D1 regulates glycosylation of type I collagen and influences collagen properties

GLT25D1 adds the monosaccharide Gal(β1-O) to procollagen's hydroxylysine residue. We investigated whether GLT25D1 influenced specific collagen post-translational modification of COL I in mHSCs and LX-2 cells. In the α1 chain isolated from WT mouse-derived mHSCs, the glycopeptides α1(501–541) were shown to contain two hydroxylated Lys: Hyl-527 and Hyl-541. The Hyl-527 residue was glycosylated by the G-Hyl glycoforms (Fig. 8A). However, the G-Hyl and GG-Hyl glycoforms were not observed in the α1 chain isolated from GLT25D1$^{+/-}$ mHSCs. The α1 chain in LX-2 cells contained three glycosylation sites: at residues α1-586, α1-594, and α1-862, while the α2 chain contained one glycosylation site at residue α2-657. However, only the α1 chain was glycosylated at site α1-586 in sh-GLT25D1 cells. Three additional glycosylation sites were observed in the OE-GLT25D1 α1 chains: at residues α1-448, α1-781, and α1-934 (Supplemental Table 4). The study results confirmed that the glycosylation of collagen from HSCs was regulated by GLT25D1.

Post-translational modifications often affect either the molecular weight or the charge of the protein. In this study, the glycosylation changes did not result in an apparent change in the electrophoretic bands (Fig. 8B). To explore whether the glycosylation affected the properties of the fibrotic ECM, collagen fiber diameters and insoluble collagen (cross-linked collagen) were investigated in BDL-induced liver fibrosis in WT and GLT25D1$^{+/-}$ mice. Collagen fibrils in the portal area viewed by SEM (Fig. 8C). After analyzed by Image-Pro Plus software, we found that heterozygous mice had fibers with larger diameters compared with WT mice (Fig. 8D). Insoluble collagen did not differ significantly between heterozygous knockdown and WT mice (Fig. 8E). SHG/TPEF imaging can characterize the architectural features of fibrosis at the individual collagen fiber level.[25] We used SHG/TPEF microscopy to capture morphological differences in liver fibrosis between WT and GLT25D1$^{+/-}$ mice. GLT25D1$^{+/-}$ mice had more long strings than WT mice. The results confirm that GLT25D1 regulated glycosylation in type I collagen and influence collagen properties.

Discussion

We previously showed that GLT25D1 was associated with liver injury, autoimmune liver disease, and nonalcoholic steatohepatitis (NASH).[19,20] However, little is known about the role of GLT25D1 in liver fibrosis and HSCs, which are mainly myofibroblast progenitor cells, and the central collagen-producing cells and key effectors in liver fibrosis.[26,31] To our knowledge, this is the first study to systematically identify the specific biological functions of GLT25D1 in liver HSCs. We found that GLT25D1 was upregulated in activated HSCs and played an essential role in HSC activation, ECM production, and collagen stabilization.

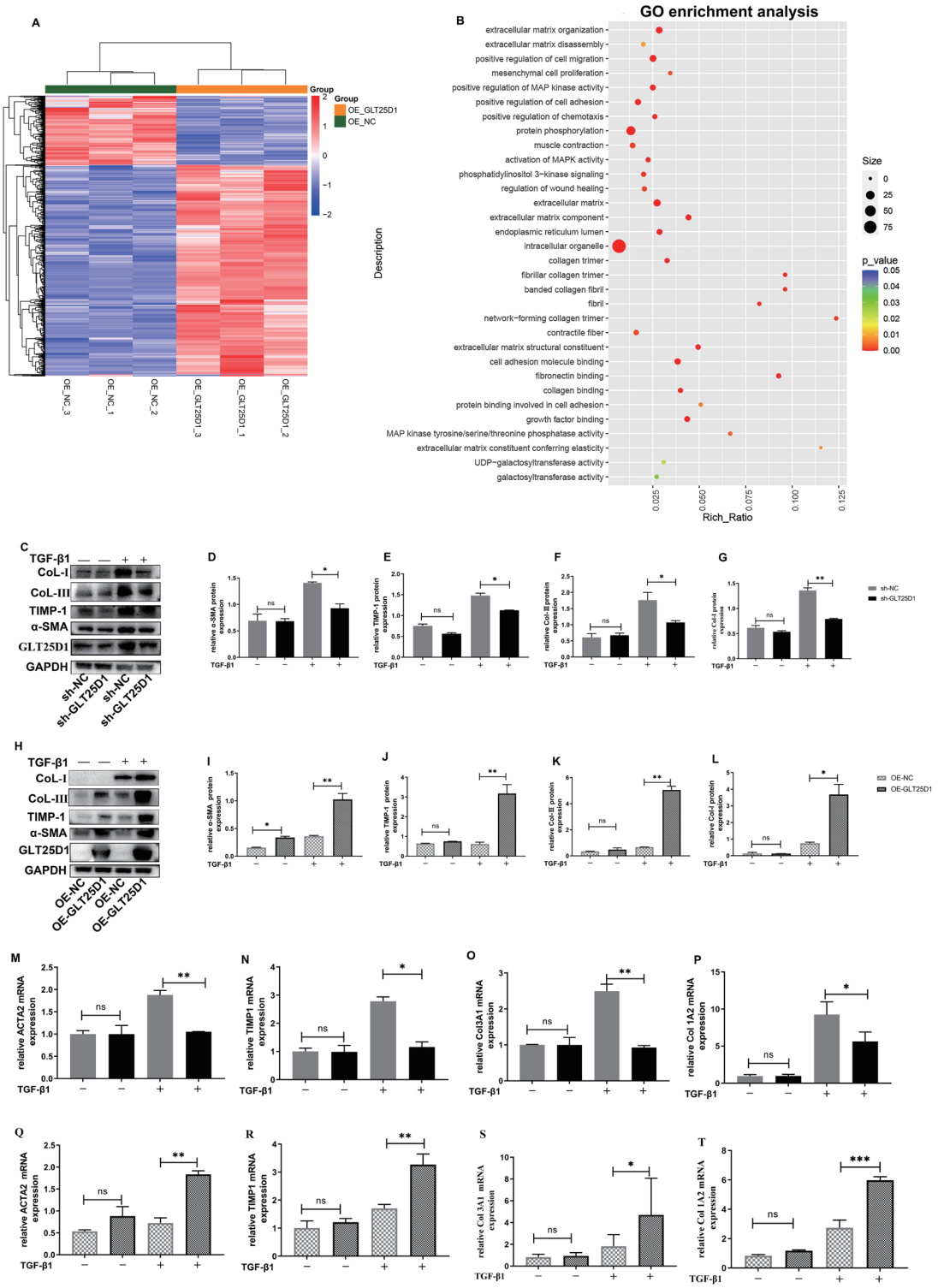

Fig. 6. GLT25D1 regulates TGF-β1-induced HSC activation and ECM production by LX-2 cells. (A) Heatmap showing genes that are differentially expressed between OE-NC and OE-GLT25D1 cells treated with TGF-β1 for 48 h. Blue represents low expression and red represents high expression. (B) GO enrichment analysis of genes in OE-NC and OE-GLT25D1 cells treated with TGF-β1 for 48 h. (C–G) Western blot analysis of the expression of fibrosis-related proteins (COL I, COL III, and α-SMA) in sh-GLT25D1 cells following 48 h of stimulation with TGF-β1. (H–L) Western blot analysis of the expression of fibrosis-related proteins (COL I, COL III, and α-SMA) in OE-GLT25D1 cells following 48 h of stimulation with TGF-β1. (M–P) Real-time PCR analysis of mRNA levels of fibrosis-related genes (*COL 1A1, COL 3A1, TIMP1,* and *ACTA2*) in sh-GLT25D1 cells following 48 h of stimulation with TGF-β1. (Q-T) Real-time PCR analysis of mRNA levels of fibrosis-related genes (*COL 1A1, COL 3A1, TIMP1,* and *ACTA2*) in OE-GLT25D1 cells following 48 h of stimulation with TGF-β1. Representative results from three independent experiments are shown. Data are means±SD. NS, not significant; *,<0.05; **,<0.01; ***,<0.001.

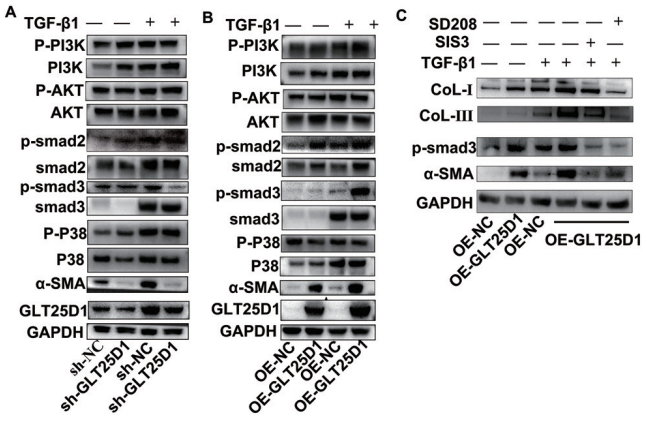

Fig. 7. GLT25D1 drives LX-2 cell activation through the TGF-β1/SMAD3 signaling pathway. (A) Western blot analysis of total PI3K, phosphorylated PI3K, total AKT, phosphorylated AKT, total smad2, phosphorylated smad2, total smad3, phosphorylated smad3, total P38, phosphorylated P38 and α-SMA protein levels in sh-GLT25D1 cells 24 h after stimulation with TGF-β1. (B) Western blot analysis of total PI3K, phosphorylated PI3K, total AKT, phosphorylated AKT, total smad2, phosphorylated smad2, total smad3, phosphorylated smad3, total P38, phosphorylated P38 and α-SMA protein levels in in OE-GLT25D1 cells 24 h after stimulation with TGF-β1. (C) Western blot analysis of p-smad3, COL I, COL III, and α-SMA protein levels in OE-GLT25D1 cells following 24 h of incubation with 3 μM of Smad3 inhibitor (SIS3) and 4 μM of TGF-βRI ALK5 inhibitor (SD208). Representative results from three independent experiments are shown.

HSCs reside in the space of Disse, between parenchymal cells and endothelial cells (EC) of the hepatic lobule.[32] In this study, GLT25D1 and α-SMA (a marker of activated HSCs) were expressed mainly in nonparenchymal liver cells in fibrotic livers. Several studies have reported that GLT25D1 is involved in collagen formation in MC3T3-E1, MEFs, SaOS-2 and collagen-producing cells.[13–15] Therefore, we concluded that GLT25D1 expression was also present in activated HSCs. We previously demonstrated that the concentration of GLT25D1 in serum from patients with cirrhosis was significantly higher than in serum from patients without cirrhosis.[33] The study results showed that GLT25D1 expression was upregulated in IHCs the cirrhotic liver. Importantly, partial deletion of GLT25D1 significantly reduced BDL-induced collagen deposition and α-SMA expression, indicating that GLT25D1 has an important role in liver fibrosis and HSC activation.

HSC activation leads it to transdifferentiate into MFBs, characterized by expression changes and specific phenotypes, including proliferation, contractility, migration, fibrogenesis, matrix degradation, chemotaxis, and inflammatory signaling.[34–36] In this study, GLT25D1 deficiency suppressed mRNA and protein expression of specific phenotype- and fibrosis-related genes in both LX-2 and mHSCs. Interestingly, GLT25D1 overexpression in LX-2 cells enhanced gene expression and the phenotypes, illustrating that GLT25D1 is required to activate HSCs.

Activated HSCs within the space of Disse migrate toward sites of inflammation, and deposit excessive ECM during

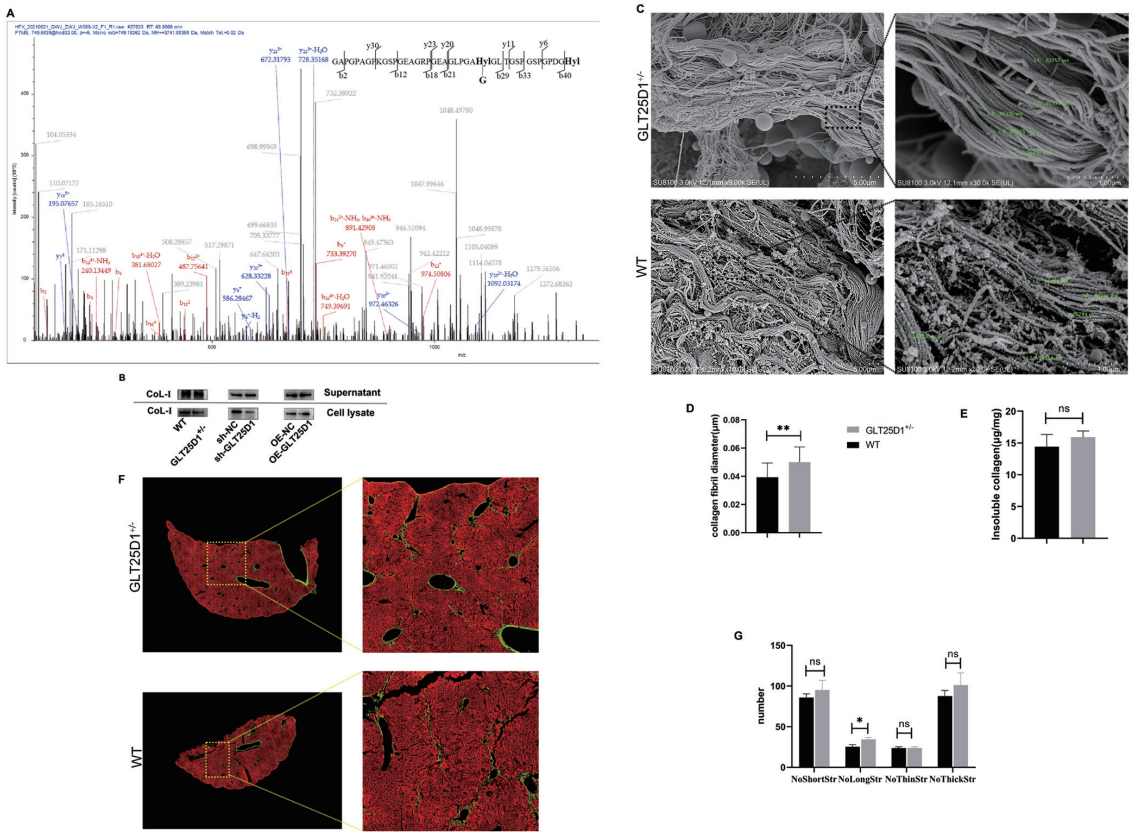

Fig. 8. GLT25D1 regulates glycosylation in type I collagen and influences collagen properties. (A) MS/MS spectra of glycopeptides. (B) Western blots showing COL I bands from LX-2 cell lysate and supernatant. (C) Collagen fibrils in the portal area viewed by SEM. (D) Collagen fibril diameters were measured in five fibrils from each group. Representative images are shown. (E) Insoluble collagen content. (F) SHG/TPEF image. Collagen is shown in green/yellow. Parenchyma is shown in red. (G) Number of short, long, thin, and thick strings. Representative results from three independent experiments are shown. Data are means±SD. NS, not significant; *,<0.05; **,<0.01; ***,<0.001.

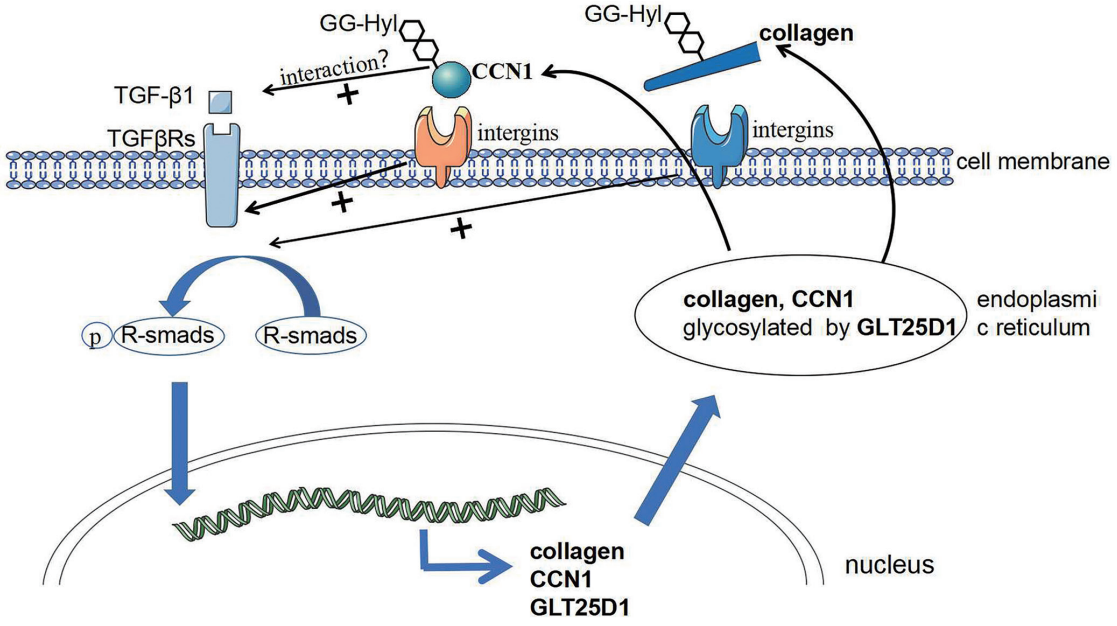

Fig. 9. Proposed model for the regulation of TGF-β1/Smad3 signaling pathway by GLT25D1 in hepatic stellate cells. Upregulation of GLT25D1 affected the glycosylation of proteins including collagen and Cellular communication network factor 1 (CCN1), which enhanced the interaction with responding receptors or TGF-β1 that synergistically activated the TGF-β1/SMAD3 signaling pathway. There is currently no evidence that proteins (TGFβRI, TGFβRII, Smad2/3/4) from the TGF-β1/SMAD pathway were glycosylated by GLT25D1. TGFβRs include type I receptor and type II receptor of TGF-β1. GLT25D1 is up-regulated in human cirrhotic liver and expressed in nonparenchymal cells. Down-regulation of GLT25D1 attenuated collagen deposition in BDL-induced liver fibrosis. GLT25D1 affected activation of primary HSCs and LX-2 cells via the TGF-β1/SMAD3 pathway. GLT25D1 regulated glycosylation in type I collagen and influenced collagen properties.

the progression of liver fibrosis.[37,38] Therefore, enhanced migration is an important aspect of GLT25D1 that contributes to liver fibrosis. Meanwhile, GLT25D1 upregulation affects cell proliferation and contractility. The high number of activated HSCs and contractibility of myofibroblasts in the fibrotic liver promote the constriction of hepatic sinusoids, resulting in blood flow and nutrient exchange.[39] Clinically, HSC contraction causes and aggravates portal hypertension that predominantly determines liver stiffness.[40,41] In this regard, GLT25D1 may be directly involved in portal hypertension formation, hence indirectly influencing liver stiffness, which correlates with liver fibrosis severity. Therefore, under conditions of chronic inflammation, GLT25D1 upregulation accelerates the progression of liver fibrosis. Baumann *et al*. reported that the loss of GLT25D1 in SaOS-2 cells induced high expression and accumulation of collagen I in the ER, although this did not result in ER stress.[13] Geister *et al*. found that, in MEFs the loss of GLT25D1 induced the accumulation of type I collagen in the cell but led to its decrease in the culture medium.[15] We obtained different results in this study. For both sh-GLT25D1 and mHSCs from GLT25D1$^{+/-}$ mice, COL I levels were significantly suppressed in the cytoplasm. This discrepancy may be due to differences in cell types, the clinical stage of the disease, the levels of GLT25D1 protein, and the knockdown and overexpression methods used. Nevertheless, it is imperative to emphasize that, in the current study, similar results were obtained using mHSC and LX-2. GLT25D1 overexpression induces the production of large quantities of collagen that need proper folding prior to secretion into the extracellular space, challenging the cell's ER folding capacity. However, it is not clear whether COL I was correctly folded and secreted.

Previous studies on GLT25D1 have focused on the structure and secretion of collagen. However, the regulation of signal pathways by GLT25D1 has not been explored. An important finding in this study is that GLT25D1 mediates the activation of LX-2 cells by enhancing the activation of the canonical TGF-β1/SMAD3 pathway. This suggests that GLT25D1, either directly or indirectly, enhances the phosphorylation of Smad3. TGF-β1-induced HSC activation is involved in several signaling pathways, including the canonical TGF-β1/SMAD and non-SMAD-dependent TGF-β signaling. Non-SMAD-dependent TGF-β signaling includes the MAPK, mTOR, PI3K/AKT, and Rho/TPase pathways.[42] The canonical TGF-β1/SMAD pathway, where SMAD3 is phosphorylated at the C-terminus, is the main fibrogenic pathway.

GLT25D1 is localized in the ER[43] while the TGF-β1/SMAD signaling pathway operates in the membrane, cytoplasm and nucleus.[42] thus, theoretically, there is no a direct interaction between GLT25D1 and proteins in the TGF-β1/SMAD pathway (TGFβRI, TGFβRII, Smad2/3/4). It is worth noting that collagen, which is regulated by GLT25D1, is also an important molecule mediating HSC activation. Col I binds to the integrin α11β1 to affect cell function.[44] However, whether the process involves the TGF-β1/SMAD signaling pathway remains undetermined. Knocking down Gal-3(galectin-3) was correlated with the downregulation of GLT25D1 in CMT cells.[45] Gal-3(galectin-3) regulates proliferation and migration of human pulmonary artery smooth muscle cells via the TGF-β1/Smad2/3 signaling pathway.[46] Therefore, Gal-3 may participate in the pathway regulated by GLT25D1. Cellular communication network factor 1 (CCN1), which is secreted by fibroblasts, is glycosylated by GLT25D1,[47] thus its function is affected by GLT25D1. CCN1 regulates the expression of genes associated with fibrosis in lung fibroblasts and is dependent on the TGF-β1/Smad3 signaling pathway.[48] This suggests that CCN1 also participates in the pathway regulated by GLT25D1 in LX-2 cells. The possible mechanism diagram was shown in Figure 9.

We confirmed that GLT25D1 regulates glycosylation (GG-Hyl, G-Hyl) in COL I from mHSCs and LX-2 cells by mass spectrometry (Supplementary Table 4). Terajima *et al* reported that this glycosylation might regulate cross-link

maturation and the growth of collagen fibrils in bone.[14] Baumann and Hennet also reported that it affects the kinetics of triple helix formation.[13] However, the content of insoluble collagen (cross-linked collagen) did not differ significantly between GLT25D1$^{+/-}$and WT mice in this study. That may be due partly to the short disease course in our fibrosis model. GLT25D1$^{+/-}$ mice had larger fibrils compared with WT mice. This is consistent with the results of previous studies showing that loss of this glycosylation induces larger mean fibril diameters compared with controls.[14,49,50] In general, collagen molecules with a higher degree of glycosylation form smaller fibrils that are involved in collagen stability.[50,51] This finding may reflect that the alteration in collagen morphology was, to some extent, regulated by GLT25D1, which may be involved in collagen degradation and the reversal of fibrosis. Thus, GLT25D1 affects liver fibrosis by altering the collagen structure.

The study has some limitations. GLT25D1 knockdown in GLT25D1$^{+/-}$ mice is not restricted to HSCs, where the biological function of GLT25D1 in hepatocytes during liver fibrosis should not be ignored[18,19] and may be accompanied by a compensatory effect of GLT25D2, another galactosyltransferase enzyme isoform.[13] Additionally, the expression of GLT25D1 in other hepatic cells remains unclear, including Kupffer cells, macrophages, cholangiocytes, and liver sinusoidal EC. Data on the role of GLT25D1 in the signaling pathway are fairly limited. When investigating collagen properties, a high purity extract of collagen was required, which need to further improve in the further study. Therefore the role of GLT25D1 in hepatic fibrosis requires further investigation.

In conclusion, our data showed that GLT25D1 regulated HSC activation and collagen stability. Additionally, GLT25D1 downregulation may alleviate liver fibrosis. Targeting GLT25D1 may be more feasible and safer than directly targeting TGF-β in liver fibrosis and offers a promising therapeutic target for treating liver fibrosis.

Acknowledgments

This work was funded by the National Science Foundation of China [No. 82170541], National Science Foundation of China [No. 81900549], Natural Science Foundation of Beijing Municipality [No. 7202071], The Capital Foundation for Clinical Characteristic Applied Research Projects [No. Z181100001718084], The Digestive Medical Coordinated Development Center of Beijing Municipal Administration of Hospitals [No. XXZ0404], The Study on Modernization of Traditional Chinese Medicine [No. 2018YFC1705700], and Capital Medical University Research Development Fund [No. PYZ20031].

Conflict of interest

The authors have no conflict of interests related to this publication.

Author contributions

Designed the experiments (HW, SW), performed experiments and wrote the manuscript (SW, MG), prepared the animal model (HW), carried out the cellular experiments (SW, YS), provided GLT25D1$^{+/-}$ mice (JY, FZ, XH, XY), performed the pathological staining (PL, XZ), and analyzed the data (LH, FX). All authors were involved in the discussions and approved the manuscript.

Ethical statement

This study was approved by the Institutional Ethics Committee of the Beijing Ditan Hospital. Written informed consent was obtained from all patients prior to obtaining liver samples. The experimental Animal Welfare Committee of Capital Medical University approved all animal procedures.

Data sharing statement

The data that support the findings of this study are available in the supplementary material and the remaining data are available on request from the authors.

References

[1] Guo YC, Lu LG. Antihepatic Fibrosis Drugs in Clinical Trials. J Clin Transl Hepatol 2020;8(3):304–312. doi:10.14218/JCTH.2020.00023, PMID:33083254.
[2] Zhou M, Wang H, Zeng X, Yin P, Zhu J, Chen W, *et al*. Mortality, morbidity, and risk factors in China and its provinces, 1990-2017: a systematic analysis for the Global Burden of Disease Study 2017. Lancet 2019;394(10204):1145–1158. doi:10.1016/S0140-6736(19)30427-1, PMID:31248666.
[3] Roeb E. Matrix metalloproteinases and liver fibrosis (translational aspects). Matrix Biol 2018;68-69:463–473. doi:10.1016/j.matbio.2017.12.012, PMID:29289644.
[4] Karsdal MA, Nielsen SH, Leeming DJ, Langholm LL, Nielsen MJ, Manon-Jensen T, *et al*. The good and the bad collagens of fibrosis - Their role in signaling and organ function. Adv Drug Deliv Rev 2017;121:43–56. doi:10.1016/j.addr.2017.07.014, PMID:28736303.
[5] Ishikawa Y, Bächinger HP. A molecular ensemble in the rER for procollagen maturation. Biochim Biophys Acta 2013;1833(11):2479–2491. doi:10.1016/j.bbamcr.2013.04.008, PMID:23602968.
[6] Scietti L, Chiapparino A, De Giorgi F, Fumagalli M, Khoriauli L, Nergadze S, *et al*. Molecular architecture of the multifunctional collagen lysyl hydroxylase and glycosyltransferase LH3. Nat Commun 2018;9(1):3163. doi:10.1038/s41467-018-05631-5, PMID:30089812.
[7] Qi Y, Xu R. Roles of PLODs in Collagen Synthesis and Cancer Progression. Front Cell Dev Biol 2018;6:66. doi:10.3389/fcell.2018.00066, PMID:30003082.
[8] Spiro RG. The structure of the disaccharide unit of the renal glomerular basement membrane. J Biol Chem 1967;242(20):4813–4823. PMID:6070267.
[9] Schegg B, Hülsmeier AJ, Rutschmann C, Maag C, Hennet T. Core glycosylation of collagen is initiated by two beta(1-O)galactosyltransferases. Mol Cell Biol 2009;29(4):943–952. doi:10.1128/MCB.02085-07, PMID:19075007.
[10] Sricholpech M, Perdivara I, Nagaoka H, Yokoyama M, Tomer KB, Yamauchi M. Lysyl hydroxylase 3 glucosylates galactosylhydroxylysine residues in type I collagen in osteoblast culture. J Biol Chem 2011;286(11):8846–8856. doi:10.1074/jbc.M110.178509, PMID:21220425.
[11] Yamauchi M, Sricholpech M. Lysine post-translational modifications of collagen. Essays Biochem 2012;52:113–133. doi:10.1042/bse0520113, PMID:22708567.
[12] Terajima M, Perdivara I, Sricholpech M, Deguchi Y, Pleshko N, Tomer KB, *et al*. Glycosylation and cross-linking in bone type I collagen. J Biol Chem 2014;289(33):22636–22647. doi:10.1074/jbc.M113.528513, PMID:24958722.
[13] Baumann S, Hennet T. Collagen Accumulation in Osteosarcoma Cells lacking GLT25D1 Collagen Galactosyltransferase. J Biol Chem 2016;291(35):18514–18524. doi:10.1074/jbc.M116.723379, PMID:27402836.
[14] Terajima M, Taga Y, Sricholpech M, Kayashima Y, Sumida N, Maeda N, *et al*. Role of Glycosyltransferase 25 Domain 1 in Type I Collagen Glycosylation and Molecular Phenotypes. Biochemistry 2019;58(50):5040–5051. doi:10.1021/acs.biochem.8b00984, PMID:31726007.
[15] Geister KA, Lopez-Jimenez AJ, Houghtaling S, Ho TH, Vanacore R, Beier DR. Loss of function of Colgalt1 disrupts collagen post-translational modification and causes musculoskeletal defects. Dis Model Mech 2019;12(6):dmm037176. doi:10.1242/dmm.037176, PMID:31101663.
[16] Webster JA, Yang Z, Kim YH, Loo D, Mosa RM, Li H, *et al*. Collagen beta (1-O) galactosyltransferase 1 (GLT25D1) is required for the secretion of high molecular weight adiponectin and affects lipid accumulation. Biosci Rep 2017;37(3):BSR20170105. doi:10.1042/BSR20170105, PMID:28428430.
[17] Miyatake S, Schneeberger S, Koyama N, Yokochi K, Ohmura K, Shiina M, *et al*. Biallelic COLGALT1 variants are associated with cerebral small vessel disease. Ann Neurol 2018;84(6):843–853. doi:10.1002/ana.25367, PMID:30412317.
[18] He L, Ye X, Gao M, Yang J, Ma J, Xiao F, *et al*. Down-regulation of GLT25D1 inhibited collagen secretion and involved in liver fibrogenesis. Gene 2020;729:144233. doi:10.1016/j.gene.2019.144233, PMID:31759980.
[19] Ye X, He L, Ma J, Li Y, Zhang M, Yang J, *et al*. Downregulation of Glt25d1 aggravates carbon tetrachloride-induced acute hepatic injury through activation of the TGF-β1/Smad2 signaling pathway. Mol Med Rep 2018;18(4):3611–3618. doi:10.3892/mmr.2018.9392, PMID:30132521.
[20] Yang J, He L, Gao M, Xiao F, Zhang F, Wang S, *et al*. Collagen β(1-O) galactosyltransferase 2 deficiency contributes to lipodystrophy and aggravates

NAFLD related to HMW adiponectin in mice. Metabolism 2021;120:154777. doi:10.1016/j.metabol.2021.154777, PMID:33865898.
[21] Ishak K, Baptista A, Bianchi L, Callea F, De Groote J, Gudat F, *et al*. Histological grading and staging of chronic hepatitis. J Hepatol 1995;22(6):696–699. doi:10.1016/0168-8278(95)80226-6, PMID:7560864.
[22] Zhao W, Yang A, Chen W, Wang P, Liu T, Cong M, *et al*. Inhibition of lysyl oxidase-like 1 (LOXL1) expression arrests liver fibrosis progression in cirrhosis by reducing elastin crosslinking. Biochim Biophys Acta Mol Basis Dis 2018;1864(4 Pt A):1129–1137. doi:10.1016/j.bbadis.2018.01.019, PMID:29366776.
[23] Modak RV, Zaiss DM. Isolation and Culture of Murine Hepatic Stellate Cells. Bio Protoc 2019;9(21):e3422. doi:10.21769/BioProtoc.3422, PMID:31993460.
[24] Huang YH, Chen MH, Guo QL, Chen YX, Zhang LJ, Chen ZX, *et al*. Interleukin-10 promotes primary rat hepatic stellate cell senescence by upregulating the expression levels of p53 and p21. Mol Med Rep 2018;17(4):5700–5707. doi:10.3892/mmr.2018.8592, PMID:29436649.
[25] Hsiao CY, Teng X, Su TH, Lee PH, Kao JH, Huang KW. Improved quantitative assessment of HBV-associated liver fibrosis using second-harmonic generation microscopy with feature selection. Clin Res Hepatol Gastroenterol 2020;44(1):12–20. doi:10.1016/j.clinre.2019.04.003, PMID:31076362.
[26] Wang Y, Vincent R, Yang J, Asgharpour A, Liang X, Idowu MO, *et al*. Dual-photon microscopy-based quantitation of fibrosis-related parameters (q-FP) to model disease progression in steatohepatitis. Hepatology 2017; 65(6):1891–1903. doi:10.1002/hep.29090, PMID:28133774.
[27] Rodriguez LG, Wu X, Guan JL. Wound-healing assay. Methods Mol Biol 2005;294:23–29. doi:10.1385/1-59259-860-9:023, PMID:15576902.
[28] Roehlen N, Crouchet E, Baumert TF. Liver Fibrosis: Mechanistic Concepts and Therapeutic Perspectives. Cells 2020;9(4):E875. doi:10.3390/cells9040875, PMID:32260126.
[29] Weiskirchen R, Weimer J, Meurer SK, Kron A, Seipel B, Vater I, *et al*. Genetic characteristics of the human hepatic stellate cell line LX-2. PLoS One 2013;8(10):e75692. doi:10.1371/journal.pone.0075692, PMID:24116068.
[30] Xu L, Hui AY, Albanis E, Arthur MJ, O'Byrne SM, Blaner WS, *et al*. Human hepatic stellate cell lines, LX-1 and LX-2: new tools for analysis of hepatic fibrosis. Gut 2005;54(1):142–151. doi:10.1136/gut.2004.042127, PMID:15591520.
[31] Jinnin M, Ihn H, Tamaki K. Characterization of SIS3, a novel specific inhibitor of Smad3, and its effect on transforming growth factor-beta1-induced extracellular matrix expression. Mol Pharmacol 2006;69(2):597–607. doi:10.1124/mol.105.017483, PMID:16288083.
[32] Sato M, Suzuki S, Senoo H. Hepatic stellate cells: unique characteristics in cell biology and phenotype. Cell Struct Funct 2003;28(2):105–112. doi:10.1247/csf.28.105, PMID:12808230.
[33] Zhang RW, Hao XH, Liu R, Zhang XJ, Ren h, Li HM, *et al*. Correlation between serum concentration of GLT25D1 and the grading of fibrosis in patients with chronic HBV infection. Chin J Gastroenterol Hepatol 2013;22(4):360–366. (in chinese). doi:10.3969/j.issn.1006-5709.2013.04.019.
[34] Friedman SL. Mechanisms of hepatic fibrogenesis. Gastroenterology 2008; 134(6):1655–1669. doi:10.1053/j.gastro.2008.03.003, PMID:18471545.
[35] Tsuchida T, Friedman SL. Mechanisms of hepatic stellate cell activation. Nat Rev Gastroenterol Hepatol 2017;14(7):397–411. doi:10.1038/nrgastro.2017.38, PMID:28487545.
[36] Getachew A, Abbas N, You K, Yang Z, Hussain M, Huang X, *et al*. SAA1/TLR2 axis directs chemotactic migration of hepatic stellate cells responding to injury. iScience 2021;24(5):102483. doi:10.1016/j.isci.2021.102483, PMID:34113824.
[37] Yang C, Zeisberg M, Mosterman B, Sudhakar A, Yerramalla U, Holthaus K, *et al*. Liver fibrosis: insights into migration of hepatic stellate cells in response to extracellular matrix and growth factors. Gastroenterology 2003;124(1):147–159. doi:10.1053/gast.2003.50012, PMID:12512039.
[38] Lee UE, Friedman SL. Mechanisms of hepatic fibrogenesis. Best Pract Res Clin Gastroenterol 2011;25(2):195–206. doi:10.1016/j.bpg.2011.02.005, PMID:21497738.
[39] Zhou WC, Zhang QB, Qiao L. Pathogenesis of liver cirrhosis. World J Gastroenterol 2014;20(23):7312–7324. doi:10.3748/wjg.v20.i23.7312, PMID:24966602.
[40] Lunova M, Frankova S, Gottfriedova H, Senkerikova R, Neroldova M, Kovac J, *et al*. Portal hypertension is the main driver of liver stiffness in advanced liver cirrhosis. Physiol Res 2021;70(4):563–577. doi:10.33549/physiolres.934626, PMID:34062072.
[41] Iwakiri Y, Trebicka J. Portal hypertension in cirrhosis: Pathophysiological mechanisms and therapy. JHEP Rep 2021;3(4):100316. doi:10.1016/j.jhepr.2021.100316, PMID:34337369.
[42] Dewidar B, Meyer C, Dooley S, Meindl-Beinker AN. TGF-β in Hepatic Stellate Cell Activation and Liver Fibrogenesis-Updated 2019. Cells 2019;8(11):E1419. doi:10.3390/cells8111419, PMID:31718044.
[43] Liefhebber JM, Punt S, Spaan WJ, van Leeuwen HC. The human collagen beta(1-O)galactosyltransferase, GLT25D1, is a soluble endoplasmic reticulum localized protein. BMC Cell Biol 2010;11:33. doi:10.1186/1471-2121-11-33, PMID:20470363.
[44] Zeltz C, Lu N, Gullberg D. Integrin α11β1: a major collagen receptor on fibroblastic cells. Adv Exp Med Biol 2014;819:73–83. doi:10.1007/978-94-017-9153-3_5, PMID:25023168.
[45] de Oliveira JT, de Matos AJ, Gomes J, Vilanova M, Hespanhol V, Manninen A, *et al*. Coordinated expression of galectin-3 and galectin-3-binding sites in malignant mammary tumors: implications for tumor metastasis. Glycobiology 2010;20(11):1341–1352. doi:10.1093/glycob/cwq103, PMID:20591828.
[46] Cao N, Tang X, Gao R, Kong L, Zhang J, Qin W, *et al*. Galectin-3 participates in PASMC migration and proliferation by interacting with TGF-β1. Life Sci 2021;274:119347. doi:10.1016/j.lfs.2021.119347, PMID:33716065.
[47] Ishizawa Y, Niwa Y, Suzuki T, Kawahara R, Dohmae N, Simizu S. Identification and characterization of collagen-like glycosylation and hydroxylation of CCN1. Glycobiology 2019;29(10):696–704. doi:10.1093/glycob/cwz052, PMID:31317175.
[48] Kurundkar AR, Kurundkar D, Rangarajan S, Locy ML, Zhou Y, Liu RM, *et al*. The matricellular protein CCN1 enhances TGF-β1/SMAD3-dependent profibrotic signaling in fibroblasts and contributes to fibrogenic responses to lung injury. FASEB J 2016;30(6):2135–2150. doi:10.1096/fj.201500173, PMID:26884454.
[49] Sricholpech M, Perdivara I, Yokoyama M, Nagaoka H, Terajima M, Tomer KB, *et al*. Lysyl hydroxylase 3-mediated glucosylation in type I collagen: molecular loci and biological significance. J Biol Chem 2012;287(27):22998–23009. doi:10.1074/jbc.M112.343954, PMID:22573318.
[50] Bätge B, Winter C, Notbohm H, Acil Y, Brinckmann J, Müller PK. Glycosylation of human bone collagen I in relation to lysylhydroxylation and fibril diameter. J Biochem 1997;122(1):109–115. doi:10.1093/oxfordjournals.jbchem.a021717, PMID:9276678.
[51] Birk DE, Fitch JM, Babiarz JP, Doane KJ, Linsenmayer TF. Collagen fibrillogenesis in vitro: interaction of types I and V collagen regulates fibril diameter. J Cell Sci 1990;95(Pt 4):649–657. doi:10.1242/jcs.95.4.649, PMID:2384532.